Elliptic flow measurement in Pb-Pb collisions using data from ALICE and applying the 2- and 4-particle Q-Cumulant methods

Lasse Albæk

June 11, 2013

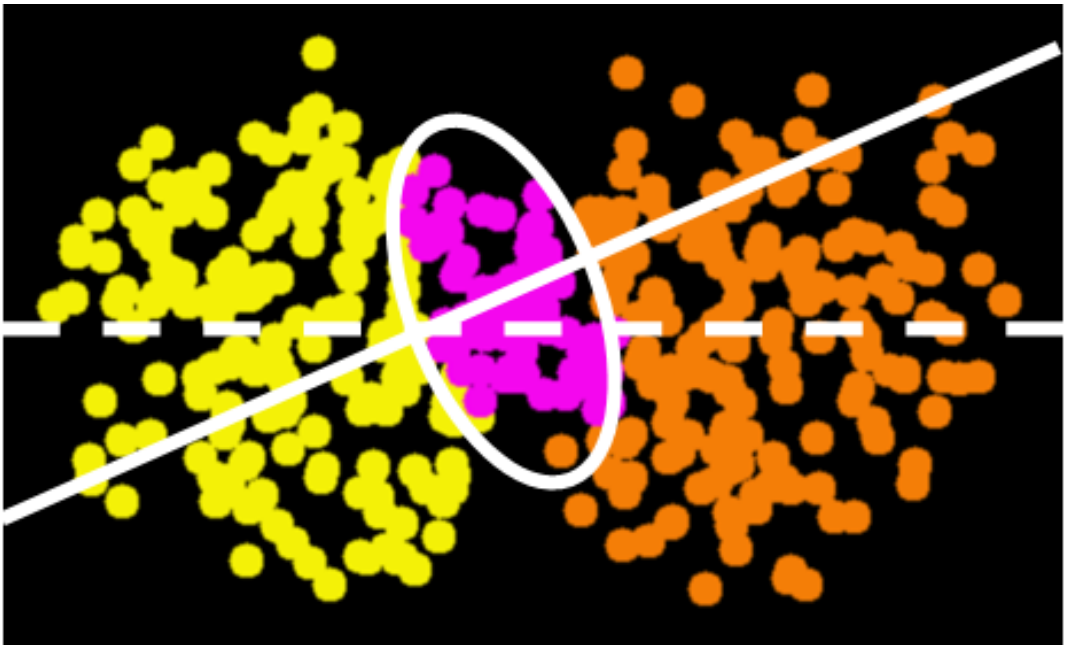

Bachelor Project at the University of Copenhagen
Supervisor: Ian Bearden
Co-Supervisor: Ante Bilandzic
CPR: 030689-1235

Date: 2013-06-11 Lasse Albæk

Abstract

The aim of this project is to measure the elliptic flow harmonic, v_2, in collisions between lead ions in the LHC at CERN at an energy per nucleon pair of $\sqrt{s_{NN}} = 2.76$ TeV. Data of the azimuthal angles of reconstructed particle tracks is taken from the TPC detector of the ALICE experiment and used with the analytical flow analysis method of Q-cumulants to estimate v_2. A new phase of matter called QGP is thought to exist at extreme energy densities, like those present in ultrarelativistic heavy-ion collisions. Elliptic flow is an important observable for determining the physical properties of QGP.

The first part of this project report describes what QGP is from the point of view of the Standard Model. Then follows an introduction to some of the important physical concepts and the origins of elliptic flow in heavy-ion collisions, after which a short description of the ALICE experiment and the workings of the TPC detector is given. In the detailed fourth part, anisotropic flow is given its formal definition and the main formulas needed for performing flow analysis using 2- and 4-particle Q-cumulants are derived. The last part provides the results of the flow analysis that confirm the presence of elliptic flow in the analyzed events and shows its dependence on both centrality and transverse momentum. v_2 is found to have its maximum value in the 40-50 % centrality interval, where it is measured to be 0.0857 ± 0.0004 with the 4-particle Q-cumulant estimate.

Dansk resume

Formålet med dette projekt er at måle koefficienten for elliptisk flow, v_2, i kollisioner mellem blyatomkerner i LHC ved CERN ved en energi pr. nukleonpar på $\sqrt{s_{NN}} = 2.76$ TeV. Data for rekonstruerede partikelspors azimutvinkler fås fra TPC detektoren i ALICE eksperimentet og bruges sammen med den analytiske beregningsmetode Q-kummulanter til at estimere v_2. En ny stoffase kaldet QGP formodes at eksistere ved ekstremt høje energitætheder der er på niveau med dem der skabes i ultrarelativistiske tung-ion kollisioner. Elliptisk flow er en vigtig observabel til bestemmelse af QGPs fysiske egenskaber.

Den første del af projektrapporten beskriver hvad QGP er set ud fra standardmodellen. Dernæst gives en introduktion til nogle af de fysiske hovedbegreber samt oprindelsen af elliptisk flow i tung-ion kollisioner, hvorefter følger en kort beskrivelse af ALICE eksperimentet og de tekniske detaljer ved TPC detektoren. I den detaljerede fjerde del gives den formelle definition af anisotropt flow og de vigtigste ligninger der bruges til flowanalyse med 2- og 4-partikel Q-kummulanter udledes. I den sidste del udlægges resultaterne af flowanalysen, der bekræfter tilstedeværelsen af elliptisk flow i de analyserede begivenheder, og viser hvordan det afhænger af centraliteten og den transversale bevægelsesmængde. Det findes at v_2 har sit maksimum i centralitetsintervallet 40-50 %, hvor den måles til at være 0.0857 ± 0.0004 med 4-partikel Q-kummulant metoden.

Contents

1 QCD and particle physics

The most successful model for describing the most elementary constituents of matter and their interactions is known as the *Standard Model* (SM) [1]. The first part of the SM is the description of the 12 known elementary fermions, the quarks and leptons, as well as the known elementary bosons via their assigned quantum numbers. The second part is the description of how these quantum numbers determine how the particles interact via the electromagnetic force, the weak force and the strong force.

The Strong Force refers to the interaction of quarks and gluons due to their *color charge*, which can be compared to the positive and negative charges of electromagnetism. The quantum mechanical model for the quarks' and gluons' interaction via the Strong Force in the SM is called Quantum Chromodynamics (QCD). It states that that there are 2 sets of 3 different color charges; blue, green, and red, and antiblue, antigreen, and antired, with each color being attracted to its anticolor, as well as the two other colors in its set. Each quark carries one color charge, hence one can have bound systems of 3 quarks, each carrying one of the three different colors of a set called baryons, or systems of one quark and one antiquark bearing a color and its anticolor called mesons. These bound systems of quarks, of which the proton and the neutron are the most common examples, are collectively called *hadrons*.

1.1 Confinement

Gluons can be compared to the photons of the electromagnetic interaction, in that they carry the strong force between quarks. However, QCD predicts that unlike the charge-neutral photons, gluons themselves have color charge. They are bicolored, bearing one color and one anticolor, that they carry between the interacting quarks, binding them together.

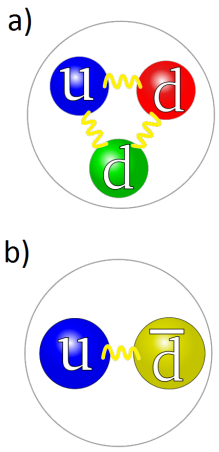

Figure 1.1: Quarks confined in a) a neutron and b) a π^+-meson

Because of their non-zero charge, gluons can interact with each other in more ways than photons. The result of these extra interactions is that the strong interaction becomes vanishingly weak at small distances, but grows very strong at large distances. Here "small" and "large" should be taken relative to the size of the typical hadron, around 10^{-15} m. This effect is known as *confinement* and is the reason why quarks are never found isolated in nature [1].

If the quarks of a hadron were to become unbound it would become more energetically favorable to simply create new quarks from the vacuum to partner up with the unbound quarks, than to let the color charges remain isolated. This is because the potential energy of the system becomes so immense, that it is greater than the rest mass of the necessary produced particles. The quarks therefore simply end up in other hadrons, the effect being that there are again no isolated quarks. This phenomenon of created hadrons is regularly observed in detectors in particle accelerators as hadron jets that are

proposed to be the signature of almost unbound quarks.

1.2 Quark-gluon Plasma

The opposite of confinement, where quarks move so closely together that the strong force becomes negligible, is known as *de*confinement. It is theorized that it should be possible to create a volume in space of such great quark density that the strong force is essentially negated [2]. This new deconfined phase of matter is called a quark-gluon plasma (QGP), and it is characterized by the quarks moving anywhere inside the plasma instead of being confined to a single hadron.

Studying QGP is important, not only because it is a newly discovered phase of matter, but also because it is a form of matter whose physical properties, like viscosity and transition temperature are almost entirely determined by the strong interaction. Determining the properties of QGP could therefore in its furthest extent have the potential to be a way of studying the strong force, and maybe determine if QCD holds true.

Producing QGP requires extreme quark densities, which in turn requires extremely high energy densities. Fortuitously, such energy densities as are thought to be necessary are produced in heavy ion collisions in some of the worlds most powerful particle accelerators like the Relativistic Heavy Ion Collider (RHIC) in Upton, New York and the Large Hadron Collider (LHC) at CERN.

2 Heavy Ion Collisions

In this project I am studying collisions between heavy ions, specifically Pb-nuclei, in the LHC recorded with the ALICE detector. In the collider tube, the nuclei are accelerated to speeds very close to the speed of light, corresponding to center-of-mass energies around $\sqrt{s_{NN}} = 2.76$ TeV per nucleon pair. At these speeds the nuclei resemble pancakes, as they are shortened 1000 times along the direction in which they are traveling [3]. Nuclei traveling in opposite directions are brought to collide, and data is collected.

When 2 particles collide in a particle accelerator, their kinetic energy in the center-of-mass frame is transformed into new particles. Since the particles are accelerated to energies corresponding to hundreds of times their rest mass, a very large amount of particles is produced. As these move away from the point of collision, they are then registered by the different detectors placed around the accelerator tube. Such a dataset corresponding to one collision is called an *event*, and the number of detected particle tracks in an event is called its *multiplicity*.

Inside the detector, position is usually given in cylindrical coordinates, with the z axis pointing along the collider tube, and the azimuthal angle ϕ circling around it. One can also define a polar angle θ which is a particle tracks inclination relative to the z axis.

2.1 Initial anisotropy and centrality

Since nuclei are only shortened along their direction of travel, they will present a non-zero area to each other, and can therefore have varying degrees of overlap

in a collision, where only the nucleons that actually hit each other react. These are called the *participants* of a collision, while the rest of the nucleons, that don't deliver energy to the reactions are called *spectators*.

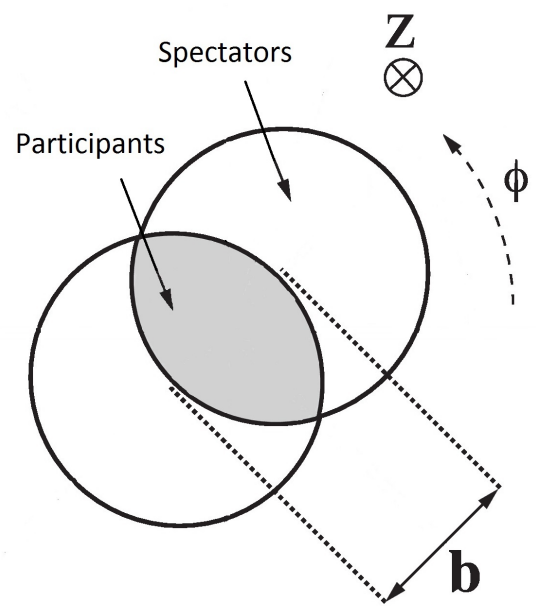

Figure 2.1

As seen in figure 2.1, if the two colliding nuclei are spherically symmetric, the initial volume containing the participants will generally be prolonged into an almond shape along an axis normal to the z axis. The QGP, if formed, will therefore have an asymmetric shape in the transverse plane, a phenomenon known as the initial spatial anisotropy [2]. This is believed to play a role in the particles' final momentum distribution as is discussed below.

Furthermore, the degree of anisotropy should depend on the amount of overlap between the colliding nuclei. The degree of overlap in a collision can be characterized by the *impact parameter*, b, which is the length of the vector connecting the centers of the two colliding nuclei. It is also shown in figure 2.1. However, the impact parameter is in general difficult to estimate event-by-event from gathered data. Instead one can try to use different methods to estimate the *centrality*, c, of the collision, which is connected to the impact parameter via

$$c = \frac{b^2}{(2R)^2}, \tag{2.1}$$

where R is the radius of the nuclei.

As c ranges from 0 to 1, it is traditionally given as a percentile. As can be seen c = 0 % means a full overlap and that the collision was therefore head-on, while c = 100 % means that the nuclei only scraped each other and that virtually all nucleons were spectators. One would therefore expect to get minimal initial anisotropy of the volume containing produced matter for c = 0 % events, as the two nuclei form a circular area in the transverse plane when colliding, while the anisotropy should be significant for mid-range to high centralities [2].

2.2 Thermalization and momentum anisotropy

To use QCD to to predict the collective behaviour of QGP requires simulating the time dependent states of every particle in the plasma. This is of course not doable in practice. What is instead done to make a model of QGP, is to treat it like a gas or fluid, and use the much simpler physical model of hydrodynamics

along with a few input parameters such as equation of state, viscosity, etc. [2]. If a QGP is created in collisions, as we hypothesize, it will be very short-lived as it will quickly expand and cool down due to the constituent particles' initial momentum. It is therefore an open question whether it will have time to thermalize, given we do not know the thermodynamical properties of the QGP.

If it does thermalize, hydrodynamics predicts that the volume containing the QGP will have a pressure that rises towards the center. This means that if there is an initial spatial anisotropy, as mentioned above, the gradient of the pressure should be largest along the direction where the volume is thinnest. Since particles are sent out with the most force where the pressure gradient is largest, the differences in pressure gradient give rise to an elliptic anisotropy in the momentum distribution of the particles, that is orthogonal to the initial spatial anisotropy. As the particles are given time to move out to the detectors, this asymmetry in momentum space is then translated into a parallel final anisotropy in coordinate space.

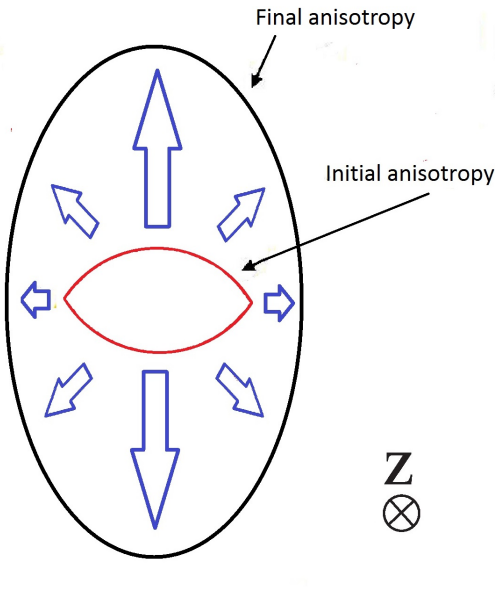

Figure 2.2

If the QGP is thermalized, one would therefore expect to detect an elliptic final anisotropy similar to the one shown in figure 2.2 [2]. This type of behaviour is called *anisotropic flow*, or more specifically *elliptic flow*, which is the subject of this study. Elliptic flow is considered to be the dominant type of anisotropic flow, and arises due to the almond shape of the initial anisotropy. How to quantify flow is explained in detail in section 4 below.

If elliptic flow is found in experiments, it can therefore be seen as evidence that the physical properties of the QGP are such that it has time to thermalize during its relatively short lifetime. This is vital information in understanding QGP and may help us evaluate our models of this new phase of matter.

2.3 Rapidity

Velocity along the beam direction, v_z, can be expressed in terms of a physical quantity called *rapidity*, y. It has the added advantage of being additive between systems moving with relativistic speeds relative to each other, unlike normal velocity, which has to be Lorentz transformed [3]. It is defined as

$$y = tanh^{-1}(\frac{v_z}{c}), \tag{2.2}$$

which reduces to $\frac{v_z}{c}$ for $v_z \ll$ c.

However, what is usually measured is the *pseudorapidity*, denoted η, which reduces to the rapidity for high energies. It can be found as

$$\eta = ln(cot(\frac{\theta}{2})). \tag{2.3}$$

It thus depends only on the track angle relative to the beam direction.

The participants in a collision should absorb each others momentum, and lose velocity, and therefore rapidity. The spectators on the other hand continue more or less unaffected, with only a small loss in rapidity.

2.4 Transverse momentum

Another important kinematic property is the *transverse momentum*, which is defined as the component of a particles momentum that is orthogonal to the beam direction,

$$p_t = \sqrt{p_x^2 + p_y^2}. \tag{2.4}$$

Transverse momentum is one of the observables measured directly in a collision. It is more physically relevant than the full momentum, p, because any momentum along the beam-line might simply be left over from the original momenta of the colliding particles, while the transverse momentum will always arise from reactions taking place at the vertex [3]. It is also easier to measure because of the way particle tracks are detected by their projection onto the x-y plane.

It is related to the pseudorapidity via

$$p = p_t \cdot cosh(\eta). \tag{2.5}$$

The physical meaning of p_t in relevance to flow is that high-momentum particles interact more than low-momentum particles. High-p_t particles can therefore be seen as having a higher probability of being thermalized, and can thus be expected to exhibit a greater degree of elliptic anisotropic behaviour, if they are analysed separately. On the other hand, the particles with the very highest momentum will have a higher probability of escaping before they are thermalized, simply because of their high velocities, and elliptic flow should therefore start dropping at some high-p_t limit. These effects will be looked for in the section holding the results below.

3 The ALICE Experiment

A Large Ion Collider Experiment (ALICE) is one of four major experiments present at the LHC particle accelerator at CERN. As the name suggests the main purpose of ALICE is to study the collisions of heavy ions, primarily Pb nuclei, at high energies. The energy per nucleon pair in heavy ion collisions is somewhat smaller than in proton-proton collisions, but because the Pb nuclei are far more massive, the energy densities at collision are generally much higher, and ALICE is therefore built to monitor high-multiplicity events.

The other major experiments present at the LHC are ATLAS, CMS and LHCb. ATLAS and CMS were both built to study proton-proton collisions at

higher energies than have previously been achievable, in order to look for new particles, like the Higgs boson. LHCb looks for CP-violation, in an effort to help explain matter-antimatter asymmetry in the Universe.

ALICE consists of a number of different detectors placed together in a cylindrical structure around the accelerator tube. They include the *Time Projection Chamber* (TPC), *Forward Multiplicity Detector* (FMD), the V0 and T0 detectors, a photon spectrometer, and others [6].

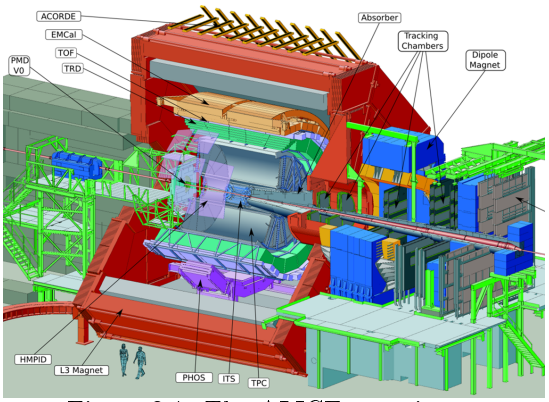

Figure 3.1: The ALICE experiment

In this project I will only use data collected by the TPC detector, and I will therefore not go into detail about the workings of the other detectors; however centrality estimates in the analysis come from the V0 detector.

3.1 TPC

The TPC is the main tracking detector at ALICE. It consists of a large enclosed volume containing a mixture of $Ne/CO_2/N_2$ gas. It has a cylindrical shape with an inner radius of 85 cm and an outer radius of 250 cm, and is 5 m in length along the beam direction. As charged particles travel through the gas they leave behind a trail of ions in their path. The ions are then drawn towards electrodes at the end plates of the TPC, and are registered as small currents. From these signals particle tracks are reconstructed, and information like position, direction of travel, and transverse momentum are gathered.

The use of only one detector for identifying particle tracks makes the analysis much simpler, as multiplicity varies greatly from detector to detector, due to their different detection mechanisms that are built for different types of particles. The TPC detector is often chosen for geometrical analysis as it has a high and almost uniform acceptance, meaning that a particle has an equal chance of being detected no matter where in the detector it is located [2]. A non-uniform azimuthal acceptance could in flow data analysis give a bias that would lead to detecting flow where there is none.

The TPC is also placed far enough away from the accelerator tube, that spectators are not detected. One of the few limitations of the TPC is that it can only detect charged particles as it relies on ionization of gas molecules.

4 Flow Analysis

If there is anisotropic flow in an event, as predicted in section 2 for thermalized QGP with an initial spatial anisotropy, the simplest and most straightforward approach to quantifying it is to do a Fourier analysis of the azimuthal distribution of particle tracks, or rather the idealized probability density function (pdf) from which the tracks' azimuthal angles are thought to be generated. The continuous particle pdf, p, as a function of the azimuthal angle ϕ, has the Fourier series expansion

$$p(\phi) = \frac{x_0}{2\pi} + \frac{1}{\pi}\sum_{n=1}^{\infty} x_n cos(n\phi) + y_n sin(n\phi), \tag{4.1}$$

where $x_0 = 1$ for a normalized distribution.

The coefficients x_n and y_n can then, due to the orthogonality of the cosine and sine functions, be found through

$$x_n = \langle cos(n\phi)\rangle\ ,\ y_n = \langle sin(n\phi)\rangle. \tag{4.2}$$

The brackets $\langle\rangle$ refer to the average taken over the distribution $p(\phi)$. The length of the vector (x_n, y_n) is denoted v_n, and is called the flow harmonic coefficient of n'th order:

$$v_n = \sqrt{x_n^2 + y_n^2}.$$

Since we are in general not dealing with continuous particle distributions, the average in eq. 4.2 turns into a sum when used in practice. And, since the sine functions all average to zero due to the mirror symmetry of the collision, we usually write [2]:

$$v_n \approx x_n = \langle cos(n\phi)\rangle = \frac{\sum_{i=1}^{M} cos(n\phi_i)}{\sum_{i=1}^{M} 1},$$

where i refers to the different individual particle tracks, ϕ_i are the measured azimuthal angles of the tracks, and M is the multiplicity of the event.

v_1 is called directed flow, and usually is not present as it corresponds to the particles having a bias towards moving to one hemisphere of the detector, rather than the other, which should not be possible in a symmetric collision.

v_2 is called elliptic flow [2], since a non-zero value of v_2 would give the particle distribution an elliptical shape. This corresponds exactly to the spatial anisotropy described in section 2, and I therefore limit my search to elliptic flow in this project.

The higher order harmonics are called triangular flow, quadrangular flow, pentagonal flow and so forth.

Now, this point was reached knowing that the symmetry plane of the event was aligned with $\phi = 0$. In general however, there are no favored azimuthal directions inside the detector, so the symmetry plane of the collision could point in any direction, and may not even be the same as the reaction plane, as illustrated by the figure on the front page. Therefore, in the more general case, one

needs to include the symmetry plane, ψ_n, which is specific for the event as well as the sought after harmonic [2], so

$$v_n = \langle cos(n(\phi - \psi_n)) \rangle.$$

This creates another problem though, since we can not look inside the accelerator tube to see the symmetry plane event by event.

4.1 Correlations

In order to get a good estimate for the flow harmonics, we therefore need an expression for v_n that is independent of the symmetry plane.

First it is noted that since the sine harmonics cancel out when averaged we can write $\langle cos(n(\phi - \psi_n)) \rangle$ equivalently as $\langle e^{in(\phi - \psi_n)} \rangle$. Second, we define the two-particle azimuthal correlation between two particles i and j as

$$e^{in(\phi_i - \phi_j)}.$$

Then, we note that in terms of these correlations, we can write the single-event estimate of the absolute square of the flow harmonic coefficient as

$$|v_n|^2 = \langle e^{in(\phi_i - \psi_n)} \rangle \cdot \langle e^{-in(\phi_j - \psi_n)} \rangle = \langle e^{in(\phi_i - \psi_n - \phi_j + \psi_n)} \rangle. \tag{4.3}$$

Here the terms ψ_n are equal as the particles are from the same event, so

$$\begin{aligned} |v_n|^2 &= \langle e^{in(\phi_i - \phi_j)} \rangle \\ &= \frac{\sum_{i,j=1, i \neq j}^{M} e^{in(\phi_i - \phi_j)}}{M(M-1)}, \end{aligned} \tag{4.4}$$

which is called the single-event 2-particle correlation with respect to harmonic n, denoted $\langle 2 \rangle$. M(M-1) is the number of different-particle combinations in the event.

The indices are chosen to be different so a particle's position is not checked for correlation with itself, as this would of course give a large positive contribution to the average, for reasons that are unrelated to the correlation of the positions of different particles and are therefore unrelated to flow.

The last equality in equation 4.3 is not trivially true. The right-hand side is an expectation value of the joint pdf of observables ϕ_i and ϕ_j. The factorization going from right to left is therefore only allowed for the parts of the joint pdf for which ϕ_i and ϕ_j are both only correlated to the symmetry plane of the event. These are then the parts we call flow. The parts of the particle pdf that are uncorrelated to the symmetry plane we call *nonflow* [2]. Nonflow can be due to several systematical effects present in a collision, as is discussed in section 4.4 below.

Through a derivation like the one above [2] one can also show that the 4-particle correlation $\langle 4 \rangle$ is an estimate of the flow harmonic to the 4th power.

$$\begin{aligned} |v_n|^4 &= \langle e^{in(\phi_i + \phi_j - \phi_k - \phi_l)} \rangle \\ &= \frac{\sum_{i,j,k,l=1, i \neq j \neq k \neq l}^{M} e^{in(\phi_i + \phi_j - \phi_k - \phi_l)}}{M(M-1)(M-2)(M-3)} \\ &= \langle 4 \rangle. \end{aligned} \tag{4.5}$$

The 4-particle correlation is of interest to us, because the correlation of the positions of 4 particles says more about the collective shape of the particle distribution than does the correlation of only 2 particles. As will be discussed below, this will make the 4-particle flow estimate less sensitive to certain kinds of nonflow. Higher order correlations like the 6- and 8-particle correlations can also be calculated and used to find flow.

One event consisting of $\sim$ 500 particle tracks is of course a statistically insignificant sample from which to make a good estimate of the flow, especially if the flow is relatively weak. The average is therefore taken over many events. The multi-event 2-particle correlation can for instance be calculated as

$$\begin{aligned}\langle\langle 2\rangle\rangle &= \frac{\sum_{m=1}^{N} M_m(M_m-1)\langle 2\rangle_m}{\sum_{m=1}^{N} M_m(M_m-1)} \\ &= \frac{\sum_{m=1}^{N} M_m(M_m-1)\frac{\sum_{i,j=1,i\neq j}^{M_m} e^{in(\phi_{i,m}-\phi_{j,m})}}{M_m(M_m-1)}}{\sum_{m=1}^{N} M_m(M_m-1)} \\ &= \frac{\sum_{m=1}^{N}\sum_{i,j=1,i\neq j}^{M_m} e^{in(\phi_{i,m}-\phi_{j,m})}}{\sum_{m=1}^{N} M_m(M_m-1)},\end{aligned} \tag{4.6}$$

where N is the number of events, and m is their indices.

Note that the event weights M(M-1) are such that each single correlation in each event counts the same towards the average. This is a reasonable, but conscious choice, which has the effect that high-multiplicity events have higher influence on the average, because the number of distinct particle pairs in an event increases geometrically with the multiplicity of the event. The higher order multi-event correlations are done in a similar way.

Multi-event correlations are a step in the right direction towards making a good estimate of the flow harmonics, but the method still has two major problems. First, correlations are relatively sensitive to nonflow. And secondly, the number of necessary calculations is so large that it is not usable in practice for large data samples, due to limited computation resources.

4.2 Cumulants

One way to adress correlations' sensitivity to nonflow is to use *cumulants* instead.

In general, if there are two variables, x_1 and x_2 with probability density functions $f_1(x_1)$ and $f_2(x_2)$, then their joint pdf, f, will have the form [2]

$$f(x_1, x_2) = f_1(x_1) \cdot f_2(x_2) + f_c(x_1, x_2),$$

where the term $f_1(x_1) \cdot f_2(x_2)$ is due to the statistically independent, or uncorrelated, parts of the pdf's, while the term $f_c(x_1, x_2)$, which we call the *genuine*

2-observable correlation or simply the cumulant, is due only to the parts of the pdf's that are correlated.

In our case, the two observables are $e^{in\phi_i}$ and $e^{-in\phi_j}$, and the average we take represents the expectation value of an observable with respect to their joint pdf. It therefore has both statistically dependent and independent parts, which are

$$\langle\langle 2\rangle\rangle = \langle\langle e^{n(\phi_i - \phi_j)}\rangle\rangle = \langle\langle e^{in\phi_i}\rangle\rangle \cdot \langle\langle e^{-in\phi_j}\rangle\rangle + c_n\{2\},$$

where $c_n\{2\}$ is the 2-particle cumulant, which can be isolated as

$$c_n\{2\} = \langle\langle 2\rangle\rangle - \langle\langle e^{in\phi_i}\rangle\rangle \cdot \langle\langle e^{-in\phi_j}\rangle\rangle. \tag{4.7}$$

Due to the random alignment of the collision symmetry plane, the expectation values of the single-particle azimuthal distributions are zero, so for the 2-particle cumulant we simply arrive at

$$\begin{aligned} c_n\{2\} &= \langle\langle 2\rangle\rangle, \\ v_n\{2\} &= \sqrt{c_n\{2\}}, \end{aligned} \tag{4.8}$$

where $v_n\{2\}$ is the 2-particle estimate of the flow harmonic v_n.

It is thus apparently not possible to improve on the 2-particle correlation, but for the higher order correlations the corrections are significant. I simply list the result for the 4-particle correlation as the derivation is a bit long [2].

$$c_n\{4\} = \langle\langle 4\rangle\rangle - 2 \cdot \langle\langle 2\rangle\rangle^2. \tag{4.9}$$

And since $\langle\langle 2\rangle\rangle = |v_n|^2$ and $\langle\langle 4\rangle\rangle = |v_n|^4$ we get

$$v_n\{4\} = \sqrt[4]{-c_n\{4\}}. \tag{4.10}$$

$v_n\{2\}$ and $v_n\{4\}$ should be understood as two independent estimates of the same physical quantity v_n. The main advantage of using $v_n\{4\}$ instead of the simpler $v_n\{2\}$ is that it should be less sensitive to several kinds of nonflow. This is because $c_n\{4\}$ looks only at the simultaneous correlation of the positions of 4 particles, which means that sources of 2-particle nonflow correlations, like resonance decays and Coulomb attraction, are largely suppressed [2]. And, by using the 4-particle cumulant instead of the multi-event 4-particle correlation, we have essentially removed the part of the 4-particle flow estimate that had a contribution from 2-particle correlations.

In calculating flow harmonics with cumulants, we make use of $\langle v_n^2\rangle$ and $\langle v_n^4\rangle$ instead of $\langle v_n\rangle$. This means that the methods have statistical biases if there are any fluctuations in results between events, which there are bound to be. These *flow fluctuations* can be shown to always give a positive contribution to $v_n\{2\}$ and a negative contribution to $v_n\{4\}$ [7].

4.3 Q-Cumulants

The problem with doing correlations is that the number of necessary computations grows geometrically with the multiplicity of an event, and can become

quite large for multiplicities around ~ 500. It would therefore solve the problem if we had a method which only had a linear dependency on multiplicity.

First, we define the Q-vector for an event as

$$Q_n = \sum_{i=1}^{M} e^{in\phi_i},$$

where M is again the multiplicity and n is still the number of a harmonic.

Q-cumulants (QC) are cumulants done analytically using Q-vectors. We note that the Q-vectors absolute square can be written as

$$\begin{aligned} |Q_n|^2 &= Q_n^* Q_n \\ &= \sum_{i,j=1}^{M} e^{in(\phi_i - \phi_j)} \\ &= \sum_{i,j=1, i\neq j}^{M} e^{in(\phi_i - \phi_j)} + M, \end{aligned}$$

as the term inside the first sum gives unity every time the indices are the same. Now the sum in the last expression is part of eq 4.4 for the single-event 2-particle correlation, and it can easily be seen that

$$\langle 2 \rangle = \frac{|Q_n|^2 - M}{M(M-1)}. \tag{4.11}$$

If this is inserted into the definition of the 2-particle multi-event correlation in the first line of eq 4.6 we get [5]

$$\langle\langle 2 \rangle\rangle = \frac{\sum_{m=1}^{N} |Q_{n,m}|^2 - M_m}{\sum_{m=1}^{N} M_m(M_m - 1)}, \tag{4.12}$$

from which one can find the 2 particle estimate of the flow, $v_n\{2\}$.

This is an analytical result that removes the problem of the geometrically increasing number of computations. This is because finding the Q-vector only requires a number of calculations proportional to the event multiplicity. As it is analytical, it also gives the exact same result as would eq. 4.6.

A similar derivation [2][5] can be done for 4-particle correlations, which gives the result

$$\langle\langle 4 \rangle\rangle = \frac{\sum_{m=1}^{N} |Q_{n,m}|^4 + |Q_{2n,m}|^2 - 2Re[Q_{2n,m}Q_{n,m}^* Q_{n,m}^*] - 4(M_m - 2)|Q_{n,m}|^2 - M_m(M_m - 3)}{\sum_{m=1}^{N} M_m(M_m - 1)(M_m - 2)(M_m - 3)}, \tag{4.13}$$

which along with eqs. 4.9 and 4.10 can be used to find $v_n\{4\}$.

4.4 Nonflow and systematical effects

Technically, nonflow is a term used to describe a type of systematical error, in which positions of particle tracks are highly correlated, but for other reasons than each being correlated with the event plane. Nonflow effects will therefore in general add to the flow estimate, and it can produce a "fake signal", so flow is detected even when none is present [7]. Important sources of nonflow include particle decays, Coulomb attraction, jets, and track splitting.

If a particle decays right before it is detected, the positions of the daughter particles will be strongly correlated. Also, if it decays close to the vertex of the collision, the particles will have a high probability of being sent out in opposite directions in the transverse plane, which also gives a strong positive correlation. Similarly, oppositely charged particles will be drawn towards each other due to Coulomb attraction, and the particle tracks of a jet are of course all strongly correlated. Track splitting is when the code that does particle track reconstruction interprets one track as two or more tracks, whose positions will of course be highly correlated, as they are in a sense autocorrelated.

Aside from nonflow there are other types of systematic effects than can influence the results of flow analysis. Some important ones are jet quenching and non-unimform acceptance.

High-momentum particles escaping from the QGP are likely to shoot out in the direction in which the volume is thinnest, due to the simple mechanics of having fewer particles to bounce off. This gives them a tendency to move aligned with the symmetry plane of the event [7]. The positions of these particles are correlated with the symmetry plane, but we would still not classify their behaviour as flow, since it has nothing to do with the properties of a thermalized QGP. This effect is called jet quenching.

Non-uniform acceptance causes "holes" in the azimuthal distribution of data, and if these holes are nonisotropically distributed, the result can be that even for an isotropic distribution, data is clustered in certain directions, which, if not corrected for, would be interpreted as flow by our data analysis framework. However, the TPC has only small areas with low acceptance, corresponding to about 10 % of the total receptive area, and they are evenly distributed, so acceptance effects should not be an issue in my results [2].

5 Results

I have carried out flow analysis on the ALICE TPC data from run 138275 in the LHC from 2010, which was the longest and most succesful heavy-ion run in ALICE, with a total of around 1 million reconstructed events. It was done with beams of Pb-nuclei with an energy per nucleon pair of $\sqrt{s_{NN}} = 2.76$ TeV.

The kinematic cuts in my analysis were a pseudorapidity range going from -0.8 to 0.8 and a transverse momentum range going from 0.2 GeV/c to 5.0 GeV/c. All centralities were included, but the analysis was carried out separately in the centrality intervals 0-5 %, 5-10 %, 10-20 %, 20-30 %, 30-40 %, 40-50 %, 50-60 %, 60-70 %, 70-80 % and 80-100 %. This was done to facilitate comparison of flow estimates for different centrality regions, while it also means that I do not have a single estimate of the elliptic flow harmonic across all centralities in my dataset. However, since elliptic flow is considered to be a geometrical quantity

that depends on the centrality a single estimate is not essential to the analysis.

Using these cuts the 4-particle estimate of the elliptic flow coefficient of my data was $v_2\{4\} = 0.0857 \pm 0.0004$ in the 40-50 % centrality region. This should be the most reliable estimate of the flow for this centrality, given the discussions in the previous sections. It should be affected very little by nonflow effects, and due to the observational conditions there should be no other systematical effect that can cause a significant bias besides the unavoidable contribution of flow fluctuations [2].

My analysis was carried out using the flow package of the AliROOT framework, as well as a few data-sorting and plotting macros that I created myself using ROOT. The data was analysed with the help of the LHC collaboration grid, where it was split into subjobs that were computed in several parts of the world.

I have taken no part in the reconstruction of events. The pseudorapidity and transverse momentum estimates in my data, as well as the azimuthal position used for flow analysis, come from the reconstruction of TPC data. The centrality estimates of each event come from the processing of data from the V0 detector.

Part of the goal of my analysis has been to attempt to reproduce the results in the first published LHC flow paper using data from heavy-ion collisions in ALICE [8]. My figures therefore use markers similar to the ones in that article in order to ease comparison.

5.1 Method

To compute the 2-particle estimate of elliptic flow I have used eq. 4.12 to find the multi-event 2-particle correlation, and then used eqs. 4.8 to find $v_2\{2\}$, while in order to calculate the 4-particle estimate I have used eqs. 4.12 and 4.13 to find the correlations and then used eqs. 4.9 and 4.10 to find $v_2\{4\}$. The multi-event averages in eqs. 4.12 and 4.13 were taken separately over each of the above-mentioned centrality intervals.

I have also made use of differential Q-cumulants, that are not described in my project, but which are a small alteration to the original formulas of section 4. They are a method that allows one to estimate the flow of a subset of particles, for instance in a certain transverse momentum range, while making use of the statistics of the entire event [2]. In this way, one receives an estimate with a statistical error akin to that of analysing the whole event, even if the subset in question doesn't hold nearly as many particle tracks.

All the errors I list are statistical errors that are due to fluctuations in observations.

5.2 Notes on ROOT and AliROOT

In my project, all data handling and data analysis was done using ROOT. ROOT is a data analysis framework made by the CERN collaboration that is object oriented, and is written in C++ [4]. It was developed and continues to be developed by a long list of contributors connected to the LHC and previous collider experiments at CERN.

AliROOT is an extension to ROOT that contains several features specific to handling data from ALICE, including the flow package that I make use of. The flow package is developed by the flow analysts connected to ALICE and

includes premade scripts that calculate the flow harmonic coefficients from the ALICE data files using a number of different methods.

5.3 Dependence on centrality

Figure 5.1 shows my results for $v_2\{2\}$ and $v_2\{4\}$ as a function of the centrality estimate of the collision for centralities up to 60 %. The filled markers are the results of doing flow analysis with all the particle tracks of the events, while for the open markers, the analysis was done separately for positive-charged and negative-charged particles, after which the average was taken. This same-charge estimate of the flow was included, because this type of analysis is less sensitive to certain kinds on nonflow. The centers of the bins are all the same, but some of the points were shifted along the x-axis for visibility.

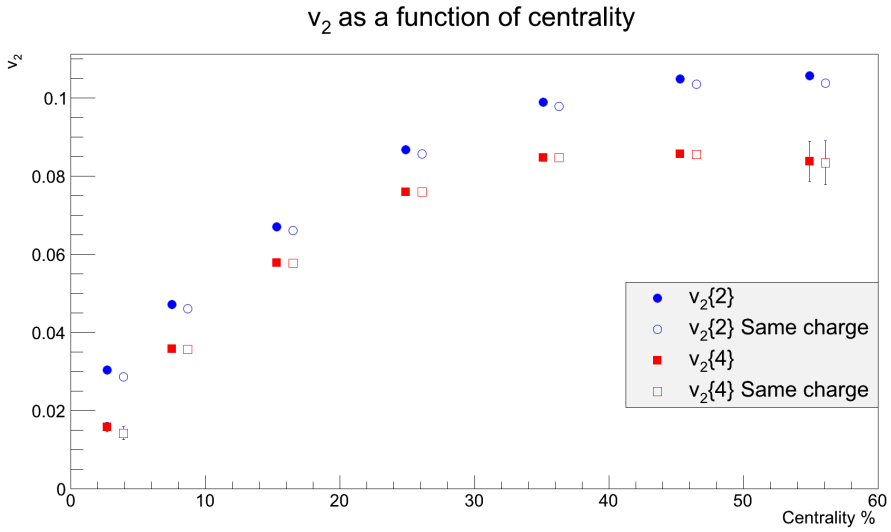

Figure 5.1

Figure 5.1 shows that in my data $v_2\{2\}$ and $v_2\{4\}$ both increase as a function of centrality, while $v_2\{2\}$ is larger than $v_2\{4\}$ for all points. The maximum for the 2-particle estimate is 0.1057 ± 0.0002 at the 50-60 % centrality interval, and for the 4-particle estimate it is 0.0857 ± 0.0004 at 40-50 % centrality. $v_2\{2\}$ seems to reach a plateau at 40-50 % centrality, while $v_2\{4\}$ flattens out already at 30-40 % centrality. The same-charge estimates correspond well to the regular ones, but the deviation is largest for the 2-particle estimates.

This behaviour is in agreement with the considerations I made about the dependence on centrality in section 2.1, where I stated that a low centrality means having little to no initial anisotropy of the volume containing the participants, as the colliding nuclei almost fully overlap. As the initial anisotropy is considered to be a perequisite for elliptic flow, this would mean that one needs a noncentral collision, i.e. with a centrality of some size, to get significant flow.

The fact that $v_2\{2\}$ is in general larger than $v_2\{4\}$ is also in agreement with the statements I made in section 4.2, that the contribution from flow fluctuations is positive for the 2-particle estimate and negative for the 4-particle estimate.

The positive deviation of $v_2\{2\}$ from its same-charge estimate is consistent with the 2-particle estimate in general being more sensitive to nonflow than the 4-particle estimate.

The $v_2\{2\}$ estimate for 80-100 % centrality, as well as the $v_2\{4\}$ estimate for 60-70 %, 70-80 % and 80-100 % centrality percentiles all have statistical uncertainties that are a magnitude higher than any of the lower-centrality intervals. Because of this I have chosen not to include this centrality range in the figure.

5.4 Dependence on transverse momentum

Figure 5.2 shows the dependence on transverse momentum of the $v_2\{4\}$ estimate for a range of centralities. These centralities were chosen because they have a clear flow signature, but with low statistical uncertainty. Estimates were originally obtained by making differential flow analysis in transverse momentum intervals of 0.1 GeV/c in width in the range from 0.2 GeV/c to 5.0 GeV/c. The results of the flow analysis were then rebinned to have uncertainties of similar magnitude in the entire range. This was necessary due to the lower statistics of the high-p_t estimates which gave the high-p_t estimates much larger statistical uncertainties than the low-p_t estimates for all centralities. Some of the points were again shifted slightly along the x-axis for visibility.

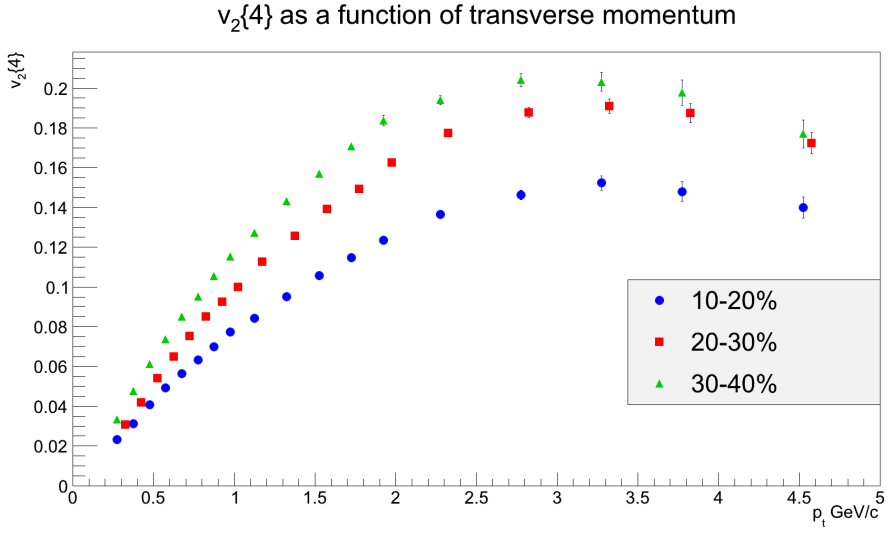

Figure 5.2

After rebinning, the figure shows a very smooth behaviour, with relatively small statistical uncertainties. It seems to indicate, that for the selected centralities elliptic flow increases as a function of momentum up to a certain point, after which it decreases slightly again. The maxima are close to each other for different centralities; the maxima for 10-20 % and 20-30 % centrality appear to be at the p_t = 3.0-3.5 GeV/c interval and the maximum for 30-40 % centrality appears to be at the 2.5-3.0 GeV/c interval. The maximum value of $v_2\{4\}$ for 30-40 % centrality is 0.204 ± 0.003.

This behaviour is consistent with the statements I made in section 2.4; that

the mid-range transverse momentum particles are more thermalized than the low-range particles, and therefore exhibit a greater degree of flow, while the highest-momentum particles escape from the initial volume too quickly to be thermalized, and therefore exhibit a smaller degree of flow. This relation is also influenced by the presence of jet quenching which gives a positive contribution to the flow estimate at high transverse momenta.

Figure 5.3 shows the dependence on transverse momentum of both the $v_2\{2\}$ and $v_2\{4\}$ estimates for centrality 40-50 %, done in the same way and using the same rebinning as in figure 5.2.

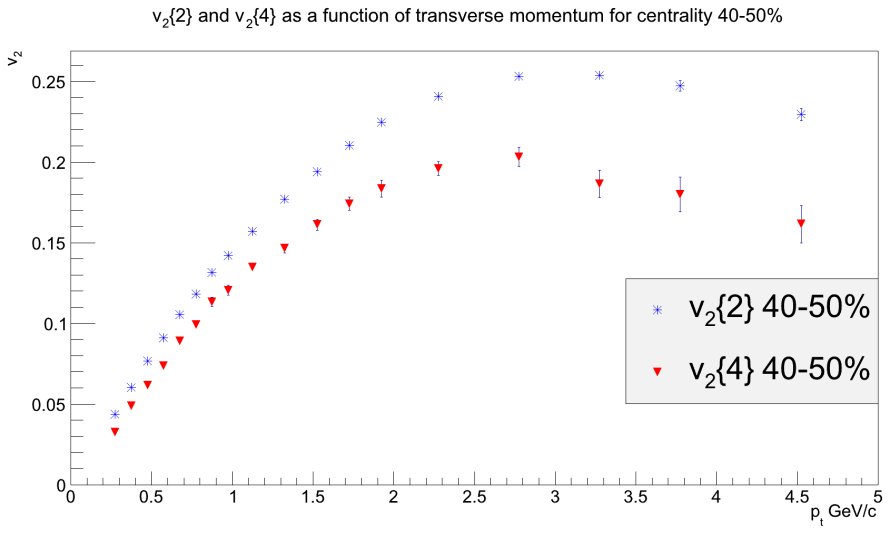

Figure 5.3

This figure shows the same dependence on transverse momentum of the 4-particle estimate as figure 5.2, and shows that this dependence is very similar for the 2-particle estimate. The 2-particle estimate has a maximum of 0.254 $\pm$ 0.002 at the 3.0-3.5 GeV/c interval, while the 4-particle estimate appears to have a maximum at the 2.5-3.0 GeV/c interval, of 0.203 $\pm$ 0.006.

Figure 5.3 also confirms what figure 5.1 showed, that $v_2\{2\}$ is in general larger than $v_2\{4\}$, but adds that this is true for the entire transverse momentum range considered.

5.5 Conclusive remarks

I have in my analysis confirmed the presence of elliptic flow in Pb-Pb collisions. My estimates for the elliptic flow harmonic have a large degree of precision for centralities below 60 %, with some of the best having a statistical uncertainty more than two magnitudes smaller than the result. However, the large difference between the 2- and 4-particle estimates indicates that the systematical error in using one or both of these methods of calculation is probably much larger than my statistical uncertainty. This systematical difference between the 2- and 4-particle estimates is consistent with $v_2\{2\}$ in general being greater than $v_2\{4\}$

due to flow fluctuations and a higher sensitivity to nonflow of the 2-particle estimate.

My results also confirm that the elliptic flow harmonic exhibits a strong dependence on both centrality and transverse momentum, as is shown in figures 5.1-5.3.

Finally, my results are for the large majority of data points consistent within uncertainties with the results presented in figures 2 and 3 of the ALICE collaboration flow paper [8]. My figures also show very much the same trends in dependencies on centrality and transverse momentum as those in the article. The statistical errors on my estimates are somewhat smaller, but that makes sense given that I use far more events than the ~ 45.000 events that were analysed in that study.

From here, a logical next step in the analysis could be to look at other harmonics, like triangular flow and quadrangular flow, in order to look for other physical effects than what is described in this project. It could also be relevant to look at v_2 estimates using 6- and 8-particle Q-cumulants to see if they correspond well with my other results.

References

[1] B.R. Martin and G. Shaw *Particle Physics*, 3rd edition, Wiley (2008).

[2] A. Bilandzic *Anisotropic Flow Measurements in ALICE at the Large Hadron Collider* (2012).

[3] J. P. Bondorf et al. *Hot and Dense Matter, Chapter 6. Relativistic Collision Kinematics* (1993).

[4] R. Brun and F. Rademakers *ROOT User's Guide* (2007).

[5] A. Bilandzic, R. Snellings, and S. Voloshin *Flow analysis with cumulants: direct calculations*, Phys. Rev. C 83 (2011).

[6] The ALICE section at CERN's homepage `aliceinfo.cern.ch/Public/en/Chapter2/Chap2Experiment-en.html`.

[7] L. Xu et al. *Decomposition of flow and nonflow in relativistic heavy-ion collisions* (2012)

[8] K. Aamodt et al. [ALICE Collaboration] *Elliptic flow of charged particles in Pb-Pb collisions at* $\sqrt{s_{NN}} = 2.76$ *TeV*, Phys. Rev. Lett. 105 (2011).

Figures 2.1, 3.1 and the figure on the front page were taken from [2]. Figure 1.1 was taken from `http://chemwiki.ucdavis.edu/Physical_Chemistry/Quantum_Mechanics/Atomic_Theory/Case_Study%3A_Quarks_and_other_sub-Nucleon_Particles`. I have made the rest of the figures myself.